

## Proposition of a bubble-particle attachment model based on DLVO van der Waals and electric double layer interactions for froth flotation modelling

Markus Buchmann <sup>1</sup>, Gülce Öktem <sup>1,2,3</sup>, Martin Rudolph <sup>1</sup>, K. Gerald van den Boogaart <sup>1,4</sup>

<sup>1</sup> Helmholtz-Zentrum Dresden-Rossendorf, Helmholtz Institute Freiberg for Resource Technology, Chemnitz Straße 40, 09599 Freiberg, Germany

<sup>2</sup> FLSmidth A/S, Vigerslev Allé 77, 2500 Copenhagen, Denmark

<sup>3</sup> Dresden University of Technology, Institute for Fluid Mechanics, D-01069 Dresden, Germany

<sup>4</sup> TU Bergakademie Freiberg, Institute for Stochastics, D-009599 Freiberg, Germany

Corresponding author: [markus.buchmann@dlr.de](mailto:markus.buchmann@dlr.de) (Markus Buchmann)

**Abstract:** The attachment of bubbles and particles represents one of the sub-processes in froth flotation among others (e.g. collision and detachment). The main interactions present at short distances in such a bubble-particle system are the van der Waals and electrostatic double layer interactions combined in the DLVO theory. In this study, the special features of the attachment process were discussed with a focus on flotation. For the van der Waals interactions, the Hamaker constants were calculated with the help of Lifshitz' macroscopic theory as a function of the separation distance for specific material combinations. A specific material system (PbS-Water-Air) was used to demonstrate the implementation of bubble-particle attachment of the proposed modelling framework. The effects of additional surfactant/collector and air layers on the solid interface were presented. This framework of layered systems showed that the sign of van der Waals interaction could be turned from repulsive to attractive without the need to extend the DLVO theory. The thickness of the layer as a function of collector adsorption between a particle and a bubble is suggested as a modelling parameter in bubble-particle attachment efficiency.

**Keywords:** attachment, froth flotation, Hamaker constant, surfactants, collectors, hydrophobic interaction

### 1. Introduction

Froth flotation is a typical example of a multi-scale process. On the lowest relevant scale for flotation, the interactions of e.g. surfactant molecules with the interface of a particle are investigated via molecular dynamics (Foucaud et al., 2021; Rath et al., 2014). The next size scale represents the bubble-particle contact (i.e. collision, attachment, and detachment), which is modelled with numerous different methods (Dai et al., 1999; Xing et al., 2017). On the level of the flotation cell, the domain is typically divided into the compartments of pulp, froth, and pulp-froth interface. To model the effects in these two distinct areas, the integral behaviour is typically modelled numerically via CFD (computational fluid dynamics) methods (Neethling & Cilliers, 2003; Schwarz et al., 2016).

To systemically model the performance of the flotation cell (i.e., recovery and concentration in the concentrate and tailings) ideally the results from the different scales must be combined. Flotation is a one-unit operation within a whole flow sheet of processes within mineral processing, where it is linked to various other processes to produce a concentrate efficiently. To understand flotation, these processes must be understood and modelled on each scale as well as having the relevant effects identified. The results of one scale must be integrated into the next scale and further information must be sent back. In the following sections, a framework for a bubble-particle attachment model is introduced and discussed with the help of a typical material example from flotation.

## 2. The bubble-particle attachment

### 2.1. Subprocess steps of attachment

In general, there are three main processes involved with the attachment of a particle to a bubble interface: 1) drainage of the intervening liquid film, 2) rupture of the interface, and 3) formation of a three-phase contact line. The time for three-phase contact line (TPCL) formation represents the time from the first collision of the bubble with the solid surface until the TPCL is formed ( $t_{TPCL} = t_{bouncing} + t_d$ ). The  $t_{bouncing}$  is the time interval until the energy is dissipated.  $t_{TPCL}$  decreases with decreasing bubble size, as the film radius decreases and therefore  $t_d$  decreases. The TPCL moves across the surface with the dewetting speed, which is a function of the thermodynamics of the three interacting interfaces as well as the roughness and other mechanical properties of the solid material (Krasowska et al., 2019). For the simplification and the possibility of quantification of the attachment process, the concepts of induction and contact time had been introduced. As the name already states the contact time represents the time of contact of the particle with the bubble. This contact is described as a sliding of the particle on the bubble's liquid/gas interface or in a more turbulent scenario a colliding of the particle with the bubble. The contact time ends when the particle slides away or bounces off. In contrast to that, the induction time represents the minimum time required for a successful attachment process. The induction time is an integral measure of physics and chemistry of the attachment process (Li et al., 2020). For approaching gas bubbles on hydrophilic surfaces, no rupture appears after the drainage process and a stable liquid film is established. (Wang et al., 2015) found in their spectroscopy studies distinctive differences in the water spectrum of thin liquid films as a function of the hydrophobicity of the solid surface, which might give further explanation on the differences of thin film stability in the bubble particle scenarios. For hydrophilic surfaces, a more ordered water structure has been observed as compared to the hydrophobic surface. These concepts referring to contact, and induction time are more related to a rather quiescent environment at relatively low turbulence intensities (e.g. in flotation columns).

The various steps of the attachment process analysed in a rather quiescent or stagnant system can differ dramatically from the behaviour in a dynamic environment (Zawala et al., 2020). A quite illustrative example is the surface boundary condition of the bubble surface (no-slip or partial slip) which depends in a dynamic environment not only on the surfactant concentrations in the aqueous phase but also on the "history of the bubble" (e.g. residue time or traveling distance) (Kosior et al., 2014). In (Wiertel-Pochopien & Zawala, 2019) the formation and the influence of a dynamic adsorption layer on the wetting film stability are described. According to (Niecikowska et al., 2012) for a dynamic system, the time for the formation of the three-phase contact line is described as the sum of the bouncing time of the bubble followed by the drainage of the wetting film. For a more turbulent system (e.g. mechanically agitated or pneumatic flotation cells), an energy-based approach is more applicable assuming an energy barrier, which has to be overcome for a successful attachment process (Pan & Yoon, 2016). The latter concept will be in focus and discussed in more detail in the following sections.

### 2.2. DLVO interactions

It is well accepted that the main interaction components at close separation distances between particles and bubbles are van der Waals (or electrodynamic) and electrostatic double-layer (EDL) interactions. These two interactions are also summarized as DLVO interactions. There are other non-DLVO interactions involved in the process (Grasso et al., 2002), but these are not subject to the considerations of this framework.

#### 2.2.1. Double layer interactions

The Poisson-Boltzmann equation describes the electrostatic potential  $\Psi$  in an ionic solution as a function of the position relative to the charged particle surface (Butt et al., 2003):

$$\epsilon \epsilon_r \nabla^2 \Psi = -e \sum_{i=0}^n z_i n_i \exp \left\{ -\frac{e z_i \Psi}{k_B T} \right\} \quad (1)$$

where  $e$  is the charge of an electron ( $1.602 \cdot 10^{-19}$  C),  $n_i$  is the number of ions per unit volume of type  $i$  in the bulk solution,  $z_i$  is the valency of ions of type  $i$ ,  $k_B$  is the Boltzmann constant ( $1.381 \cdot 10^{-23}$  J/K),  $T$  is

the temperature in K,  $\epsilon_0$  is the permittivity of the vacuum ( $8.854 \cdot 10^{-12} \text{ C}^2/\text{J}/\text{m}$ ) and  $\epsilon$  is the dielectric constant (the relative permittivity) of the medium (for water this value is about 80). This equation represents the basis for the Gouy-Chapman theory of electrical double layers (solvent is a structureless continuum, ions are point charges, the potential of mean force and the average electrostatic potential are identical), which is valid in a rather wide field (down to the separations of a few nanometres). The Derjaguin approximation allows to derive the force between two spheres as  $F(h) = 2\pi R_1 R_2 / (R_1 + R_2) G(h)$ . Here,  $R_1$  and  $R_2$  represent the radii of the spheres. The first term on the left side represents the geometric factors of the interacting bodies (also available for other geometries) and  $G(h)$  represents the Gibbs interaction free energy per unit area of two parallel plates, which are separated by a distance,  $h$ , equal to the distance between the two spheres. If the potential in the overlapping layers of the two spheres is small, the Debye-Hückel linearization can be applied to describing the potential ( $d^2\psi/dx^2 = \kappa^2\psi$ ), where  $\kappa$  is the Hückel constant (reciprocal length) and is given by  $\kappa = ((2 \cdot N_A \cdot e^2 \cdot I) / (\epsilon_0 \epsilon k_B T))^{0.5}$ . Here  $N_A$  represents the Avogadro constant ( $6.02214129 \cdot 10^{23} \text{ mol}^{-1}$ ) and  $I$  is the ionic strength in mol/l. A rather important but complex concept represents the regulation, which implies that the charge and/or the potential change during the approach process when the distance  $h$  is reduced (Lyklema & Duval, 2005). There are many approximations for the calculation of the EDL interactions mostly assuming low surface potentials and the above-mentioned simplifications (Carnie & Chan, 1993; Chan et al., 1976; Hogg et al., 1966). For the following calculation of the potential based on EDL a simplistic approach is chosen, assuming a constant charge of the particle and the bubble surfaces (Yoon & Mao, 1996):

$$V_E(h) = \frac{\pi \epsilon_r \epsilon_0 d_p d_b (\psi_p^2 + \psi_b^2)}{2(d_p + d_b)} \left( \frac{\psi_p^2 \psi_b^2}{\psi_p^2 + \psi_b^2} \ln \left( \frac{1 + \exp(-\kappa h)}{1 - \exp(-\kappa h)} \right) + \ln(1 + \exp(-2\kappa h)) \right) \quad (2)$$

where  $d_p$  and  $d_b$  represent the particle and bubble diameter, respectively. The surface potential of the bubble  $\psi_b$  and the particle  $\psi_p$  were kept constant in the following calculations at -0.01 V and -0.03 V, respectively, as we focused on the effect of the van der Waals interactions assuming here that the collector layer does not affect the particle surface potential. Further, the ionic strength was set to 0.1 mol/l. The chosen values of the surface potential imply a repulsive character for the EDL interactions in the exemplary calculations of the investigated bubble-particle system. This study was focused on changing the van der Waals interactions when certain surface layers are influencing the Hamaker constant, as shown below and hence it is not the purpose here to vary the surface potentials.

### 2.2.2. Van der Waals interactions

Lifshitz' theory of van der Waals forces is relying on macroscopic quantities to describe the electromagnetic fluctuations in condensed media, which are responsible for the interactions (Lifshitz, 1956; Parsegian, 2006). The key quantity is the complex permittivity of each material. This represents a frequency-dependent property with a real and an imaginary part. The Hamaker function  $A(h)$  for the interaction between macroscopic materials L and R, separated by medium m of thickness  $h$  can be calculated with the help of material-specific spectral data (Ninham & Parsegian, 1970). This approach can be extended to a layered system describing the interaction in a system of L and R assuming additional coatings on these materials (Parsegian & Ninham, 1973). For more details and relevant material data we here refer to our previous paper Weber et al., 2021). These material-specific Hamaker functions are used for the calculation of the potential due to van der Waals interactions, including the retardation effects, in the respective particle-bubble system (Yoon & Mao, 1996):

$$V_D(h) = \frac{A(h) d_p d_b}{12h(d_p + d_b)} \left( 1 - \frac{1 + 2bl}{1 + b \frac{c}{h}} \right) \quad (3)$$

where  $c$  is the speed of light in a vacuum ( $\approx 3 \cdot 10^8 \text{ m/s}$ ),  $b$  and  $l$  are constants ( $b = 3 \cdot 10^{-17} \text{ s}$ ;  $l = 3.3 \cdot 10^{15} \text{ s}^{-1}$ ) as found in (Butt et al., 2003).

### 2.2.3. Calculation of energy barrier

The total potential energy between particle and bubble ( $V_T$ ), as a function of distance ( $h$ ), is the sum of the individual contributions from van der Waals and electrostatic interactions according to the DLVO theory:

$$V_T(h) = V_E(h) + V_D(h) \quad (4)$$

The energy barrier in the respective system is represented as the maximum of the total energy:

$$E_B = \max (V_T(h)) \quad (5)$$

With the help of the kinetic energy approach ( $E_k=0.5mv^2$ ) the energy barrier can be transformed to a critical particle velocity  $v_p$ , which is necessary to overcome ( $E_B$ ) for successful particle-bubble attachment: ( $E_k \geq E_B$ ).

### 3. Discussion

#### 3.1. Aspects in flotation

For a detailed understanding of the attachment process, it must be emphasized that the process is influenced by the specific chemistry of the respective flotation system. The previous sections described the main interactions and main subprocesses involved in all attachment processes. Nevertheless, specific surfactants, chemical interactions, and varying parameter ranges will influence the individual attachment process for different material systems. We have identified different main material systems (e.g. flotation of quartz, semi soluble salt-type minerals, iron oxides, sulfides, and graphite) influencing the attachment interaction mechanisms. This compilation discusses a limited selection of effects for one specific material example to show the complexity of the process. It is by no means complete and might be extended by certain specific material systems.

A prominent example of the attachment process governed predominantly by electrostatic forces is the flotation of quartz. Quartz is a dominant gangue mineral present in practically all metal ores and coal. The ores are cleaned from quartz by a reverse cationic flotation (anionic is also possible). For the flotation of quartz, the main collectors represent quaternary ammonium salts. In distilled water the quartz surface is negatively charged, the same appears for the bubble surface. Further, the quartz surface is hydrophilic (or slightly hydrophobic) in distilled water. From this, it follows that for the destabilization of the wetting film between particle and bubble a charge reversal and/or a hydrophobization of the quartz is necessary (Wiertel-Pochopien & Zawala, 2019). For low concentrations, the cationic surfactants will preferentially adsorb in the gas/liquid interface, causing a charge reversal. At higher concentrations, the surfactants will adsorb at the solid/liquid interface as well, increasing its hydrophobicity (Zawala et al., 2020). In this case, the increase in surfactant concentration alters the system properties and this affects the kinetics of the liquid film drainage. A possible change of the predominant film rupture mechanism is proposed for such systems depending on the surfactant concentration from fluctuation waves (for hydrophilic surfaces and influence of attractive forces) mechanism towards cavitation or nucleation mechanism (for hydrophobic surfaces with nanobubbles). For the range of low concentration of surfactants, the  $t_{TPCL}$  shows a rapid decrease with the increase of concentration indicating an electrostatically driven liquid film rupture (increasing amplitude of fluctuation waves due to increase in force) (Kosior et al., 2015; Zawala et al., 2017). These explanations for the flotation of a quartz system represent an adequate example to show the influence of specific material aspects on the flotation and especially the attachment process.

Other prominent material groups together with their respective surfactant system showing specific chemical effects, which might influence the bubble-particle attachment mechanisms are sulfides (Albjanic et al., 2012, 2011; October et al., 2020; Sarvaramini et al., 2016; Xianchen Wang & Zhang, 2020), semi-soluble salt type minerals (Tang et al., 2020; Wang & Zhang, 2020; Yang et al., 2020) and iron oxides (Joseph-Soly et al., 2015; Ma, 2012; Pattanaik & Venugopal, 2018).

Liberation, as well as the size distribution of mineral particles represent important parameters in the flotation of a real ore, which have a direct influence on the particle-bubble attachment (Albjanic et al., 2015; Jameson, 2012). More precisely, the degree of surface liberation of the mineral component, which is targeted in flotation, is a factor determining the result of the flotation process. In many scientific modelling approaches, looking in detail at various micro processes, this property is not included. In fact, the mineralogical structure, associated liberation characteristics, and combined grinding behaviour of the material influence the flotation process dramatically. In this sense, modelling of the flotation process cannot be isolated from the upstream mineral processing operations, which is mostly a grinding process but needs to be considered together (Grano, 2009; Zhang et al., 2021). Therefore, the "history of the particle" is of high significance for flotation and especially for the attachment process. The "history of the particle" is not only to be focused on within the flotation cell (e.g. agglomeration of small particles,

particles dropping back from the froth phase into the pulp phase), but also prior to thereof (e.g. upstream processes). Further, the particle shape and the particle roughness should be mentioned within this context, potentially showing effects on the attachment process (Güven et al., 2015; Vaziri Hassas et al., 2016; Zhu et al., 2020).

### 3.2. Layered Systems

For the considerations of the particle-bubble interactions, one reasonable simplification is the approach of a layered structure. In (Doshi et al., 2005; Mittal & Hummer, 2008) the applicability to real systems of such layered systems as shown in Fig. 1 has been indicated. From left to right there is a solid layer representing the particle, a surfactant layer with the thickness  $l_1$ , a gas-enriched water layer extending over a length of  $l_2$  and the bulk water phase.

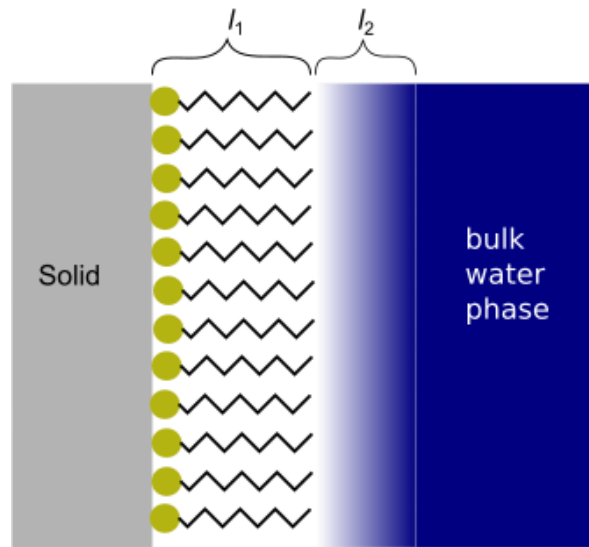


Fig. 1. Layered structure of the solid water interface

The thickness of layer  $l_1$  depends on the molecular nature of the surfactants and their adsorption configuration. This part of the layer shows a static character and has an approximately fixed size depending on the surfactant molecules and could be linked to a measure such as Young's contact angle. The adjoining layer  $l_2$  is often referred to as an interfacial gas enrichment (IGE) and shows a reduced density as compared to the bulk water phase. This layer is formed by the dissolved gas in the bulk water phase to which it has no fixed border. It is assumed to show a gradual transition to the bulk water phase with an increasing density. Further, this interface shows a fluctuating behaviour, which is described by density fluctuations, also referred to as capillary waves, in this area. The quantitative size range of this IGE is a function of the partial pressure of the dissolved gas within the bulk water phase and is not imperatively made of air, but any gas that is present in that specific system. According to (Doshi et al., 2005) the thickness of the described IGE is in the range of 0.1 nm for untreated aerated water. For calculation of the Hamaker constant including  $l_1$  and  $l_2$  we refer to our previous work containing several methods for calculating the Hamaker constant by Lifshitz's approach, including the calculations of Hamaker function in layered systems. The thicknesses of the collector layer  $l_1$  and the interfacial gas enrichment  $l_2$  are found in the complex equations of the Hamaker constant as a part of optical reflection coefficients.

Following the hydrodynamic theories and assuming a layered structure according to Fig. 1, the stability of the thin film between solid surface and bubble is a function of thickness fluctuations (density fluctuation or capillary waves), of which the wavelengths can be altered under the influence of interparticle forces (electrostatic, van der Waals). When a certain limit is reached and waves from neighbouring interfaces overlap (interferential concept) a hole is formed, the film is perforated and the critical film thickness is reached  $h_{crit}$ , which represents the (measurable) mean film thickness at that point. Under the described assumption of the presence of these wave-like density fluctuations, it is useful to speak of a critical wavelength  $\Lambda_{crit}$  (Vrij & Overbeek, 1968). Under certain simplifying

assumptions (e.g. other forces than van der Waals neglected) this can be calculated via  $\Lambda_{\text{crit}} = 2\pi(\pi \gamma h^4/A)^{0.5}$ , where  $h$  is the width of the film,  $\gamma$  is the surface tension and  $A$  is the Hamaker constant. From this simple function, it follows that with increasing van der Waals forces, as well as with decreasing surface tension, the critical wavelength for rupture is lowered. In the following calculations, an exemplary system of PbS-Water-Air was chosen. For such a layered system, the Hamaker functions for a varying surfactant layer thickness (see Fig. 2) and an additional IGE layer (see Fig. 3) were calculated as described in Section 2.2. To our knowledge, spectral data of common collectors are not available. Therefore, we used decane to represent the hydrophobic tail of a collector. The chosen values for the thickness of the surfactant layer must be understood as average values describing an integral value over the whole solid interface. The values of the surfactant layer thickness  $l_1$  are linked to the wettability describing parameters (contact angle or surface energy) via the concept of surface coverage ( $\Gamma$ ) of the surfactant molecules. The higher  $\Gamma$ , the higher is the hydrophobicity of the surface. The maximum thickness of  $l_1$  is in the range of the length of a decane molecule ( $\sim 2$  nm). The lower values represent a lower coverage of the surface assuming a linear correlation of the thickness  $l_1$  with the adsorption coverage up to the maximum. In addition, there is a dependency of the surface coverage on the concentration of surfactant molecules in the flotation suspension, which allows the calculation of the hydrophobicity as a function of surfactant concentration based on these considerations.

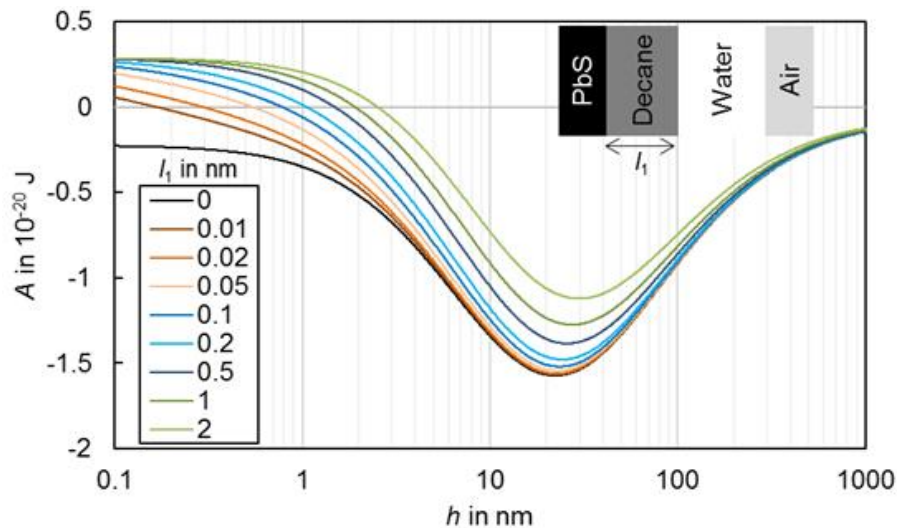


Fig. 2. Hamaker functions in layered systems: PbS with adsorbed decane layers of indicated thickness  $l_1$ , interacting with air across water

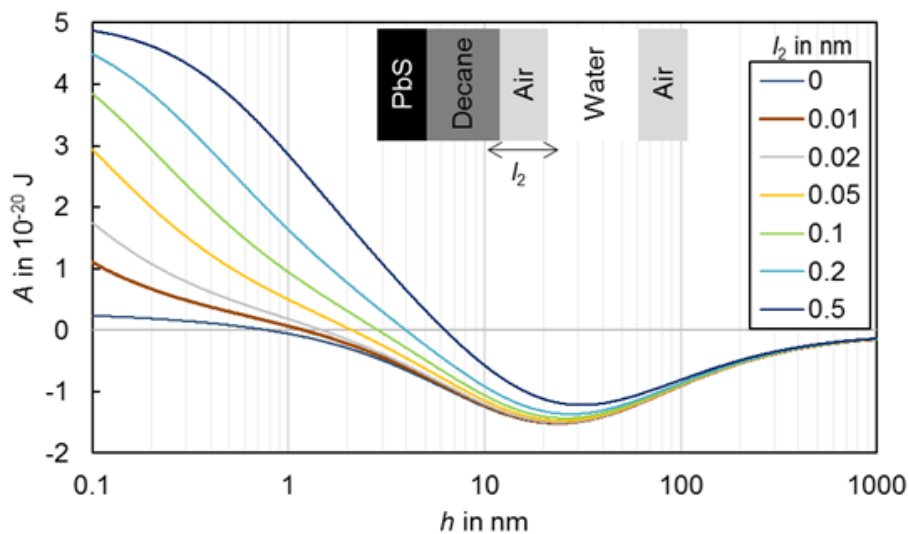


Fig. 3. Hamaker functions in layered systems: PbS with adsorbed constant decane layer of  $l_1 = 0.1$  nm and layers of air with indicated thickness  $l_2$  interacting with air across water

For the pure system only consisting of PbS-H<sub>2</sub>O-Air, the Hamaker function shows a purely repulsive character over the entire distance  $h$ . By adding a surfactant and/or an IGE, the Hamaker function is shifted to an attractive character. According to the surface structure shown in Fig. 1, and considering the influence of gas saturation of the water phase, (Krasowska et al., 2019) showed that the stability of the wetting film and the time for attachment decreased for experiments with air saturated solutions (by two orders of magnitude compared with degassed water). Similar observations were made with a solid surface of increasing surface roughness (Krasowska & Malysa, 2007a, 2007b).

As it is shown in Fig. 3, surfactant and gas layers/bubbles can change the acting van der Waals interactions dramatically. The existence of gas films/bubbles and surfactant layers on solid surfaces immersed in water can explain the overall attraction of bubbles and particles for originally repulsive material systems. Given that the range of the surfactant gas layer is thicker than the extent of the electrical double layer, the van der Waals interactions are expected to be dominantly attractive for the system in consideration. The formation of the discussed gas layers is promoted by hydrophobicity and/or physical or chemical surface heterogeneity (Snoswell et al., 2003). Following the context of the presented dependencies for attractive Hamaker functions, the overall attraction of hydrophobic particles and air bubbles can be explained within the context of the classical DLVO theory (Mishchuk et al., 2006; Mishchuk, 2011).

### 3.3. Energy barrier

The total interaction potential  $V_T$  for an exemplary particle-bubble system was calculated using Eq. 2, 3, and 4. Further, the van der Waals interactions were calculated based on the Hamaker functions from Section 3.2. In Fig. 4,  $V_T$  is shown as a function of the separation distance between particle and bubble having a constant size ( $d_b = 1000 \mu\text{m}$ ,  $d_p = 100 \mu\text{m}$ ) with varying thickness of the surfactant layer. For the pure system without any surfactant,  $V_T$  shows a steady increase with decreasing  $h$ . A similar trend is visible for surfactant layers with a quite low thickness ( $\leq 0.05 \mu\text{m}$ ), but with slightly decreasing values of  $V_T$ . For higher thickness values, a clear maximum appears above a distance of 0.1 nm. These results imply that  $V_T$  can be decreased significantly within the originally repulsive system with only a surfactant layer on the particle.

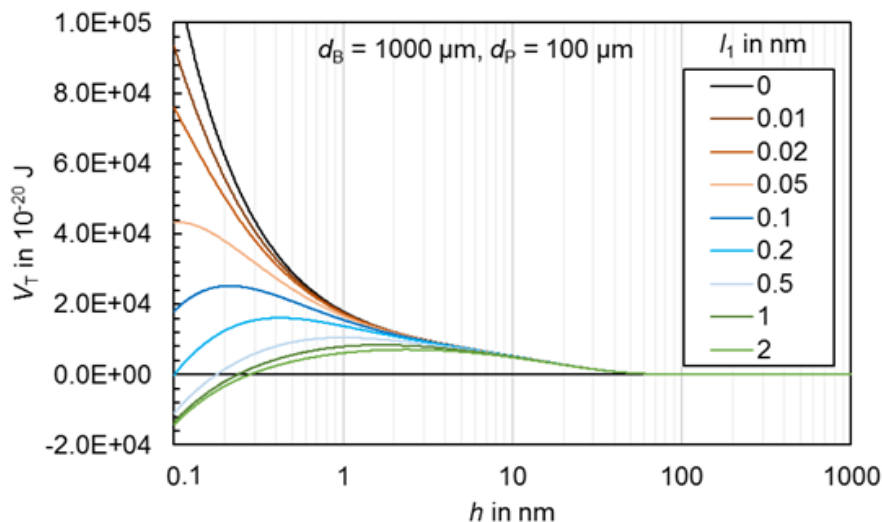


Fig. 4. Total Potential  $V_T$  as a function of the distance  $h$  between particle and bubble with a variation of surfactant layer thickness  $l_1$

For the same system but with an additional IGE layer, the  $V_T$  trends, dropping further with increasing thickness of the IGE layer, are shown in Fig. 5. Additionally, the location of the maximum shifts quite significantly to higher values of  $h$  as compared to the case with only the surfactant layer on the particle surface.

Based on the computed total interaction values  $V_T$ , the energy barrier  $E_B$  can be calculated by Eq. 5. This was done for the investigated system as a function of the particle size and the bubble size for the various surfactant layer thicknesses. These  $E_B$  values can be transferred to minimum particle velocities

necessary for a positive attachment as shown in Fig. 6. Firstly, there is a significant drop in  $v_p$  with increasing particle size. The right-sided diagram in Fig. 6 shows the case of a standard average bubble size of 1000  $\mu\text{m}$ , whereas the left and middle ones show the cases of quite low bubble sizes of 100  $\mu\text{m}$  and 10  $\mu\text{m}$  (referred to as microbubbles). For the cases with no surfactant layers, the values of  $v_p$  can only be understood theoretically as  $E_B$  cannot exist due to the asymptotic behaviour of  $V_T$ , in which no attachment will occur. There is a shift to a lower  $v_p$  with decreased bubble size, but this correlation is not as significant as in the case of particle size variation. Further, the bubble size effect is less pronounced for small particle sizes and increases with increasing particle size.

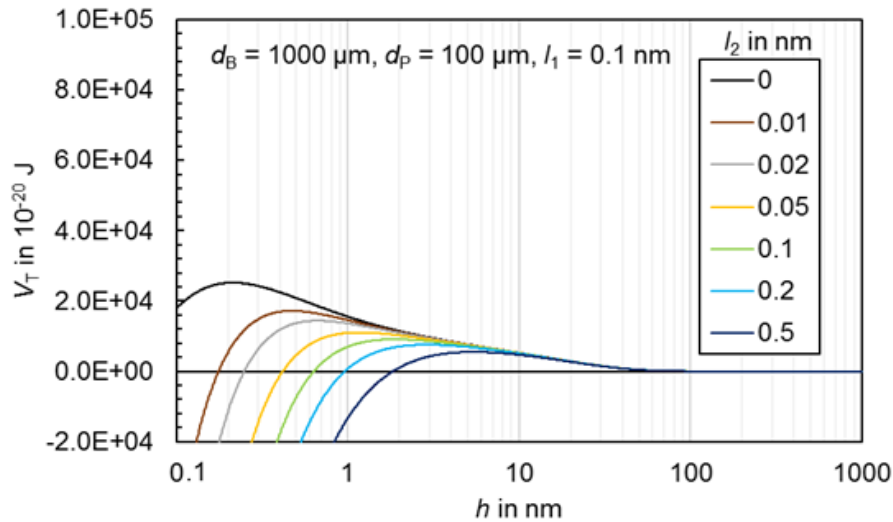


Fig. 5. Total Potential  $V_T$  as a function of the distance  $h$  between particle and bubble with a variation of air layer thickness  $l_2$  and a constant thickness  $l_1 = 0.1$  nm

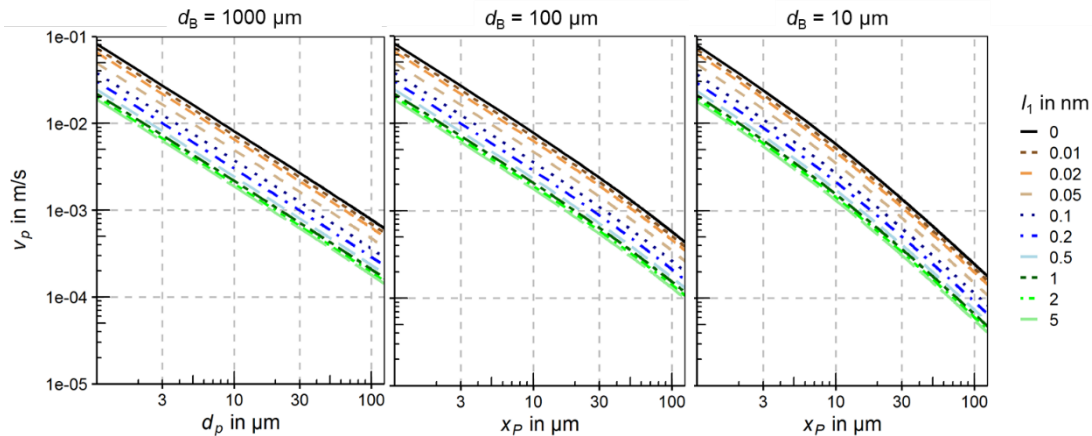


Fig. 6. Critical velocity  $v_p$  as a function of particle size  $x_p$  and thickness of decane layer  $l_1$  for three different bubble sizes (left:  $d_B = 1000$   $\mu\text{m}$ ; middle:  $d_B = 100$   $\mu\text{m}$  and right:  $d_B = 10$   $\mu\text{m}$ )

The calculations for  $v_p$  assumed particles only consisting of PbS, which justified the application of a relatively high density of 7.4  $\text{g}/\text{cm}^3$  for the calculations. For most other minerals in flotation, the density would be significantly lower, leading to relatively higher values of  $v_p$ . Furthermore, the assumption of particles consisting of only one mineral phase is only applicable for highly liberated particles. This might be true for relatively small particle sizes (depending on the mineral grain sizes), but not for coarser particles. In the simplest case, this changes the actual particle density and will further lead to varying material-specific interactions (van der Waals as well as EDL interaction will consequently change).

### 3.4. Further effects and outlook

In this section, some additional effects are discussed, which represent potential extensions of the presented basic model of particle-bubble attachment. The approach speed of the particle changes in the

vicinity of the bubble. In the simplest case, assuming only a pressure gradient, the resulting velocity of the particle changes only due to the density difference between liquid and particle ( $v_1 = v_l (1 - \rho_l / \rho_p)^{0.5}$ ) where  $v_l$  is the speed of the liquid,  $\rho_p$  and  $\rho_l$  the particle and the liquid velocity, respectively.

For additionally assuming traction within the system, the resulting particle velocity is additionally depending on a traction coefficient ( $v_2 = v_1 \cdot \exp(-0.5c_1 t)$ ), where  $c_1$  is the traction coefficient for  $\delta / \delta t \Delta v = -c_1 \Delta v$  and  $t = 2s / (v_1 + v_2)$  with  $s$  the size (thickness) of the hydrodynamic boundary layer.

Assuming a deformable bubble interface, the bubble diameter needs to be corrected for the case of a particle approaching the bubble interface. According to the pressure equilibrium at the bubble boundary, where the Laplace pressure of the bubble must stop the approaching liquid, we have a dynamic bubble diameter  $d_{bd}$  ( $1/d_{bd} = (v_1^2 \rho_l) / (4\gamma) + 1/d_b$ ), where  $d_b$  is the static bubble diameter and  $\gamma$  is the surface energy of the bubble.

For fine particles (<20  $\mu\text{m}$ ) the bubble loading capacity might be a restricting parameter for the attachment process. As fine particles would lead to relatively high loading of the bubble interface, the attachment of further particles would be hindered, and the first-order kinetics eventually changes to zero-order kinetics (Neethling et al., 2019).

Further, the actual surfactant concentration can be linked to the present layer thickness in the system. This is possible with the help of a specific Langmuir adsorption isotherm for the applied surfactant molecules. This would help to understand the effects of varying surfactant concentrations in specific flotation systems. In addition, the layered system can be extended to other substances to show a shifting of the values of Hamaker constants towards negative, i.e. stronger van der Waals attraction, such as in the case in which the interaction between an oil-covered particle and an oil-covered bubble, or an additional layer stemming from surfactant (frother) adsorption in the bubble surface, is considered.

The mentioned points represent only a selection of relevant points of a huge number of different parameters affecting the particle bubble attachment, which will be included in the model at a later stage. It is important to remind that this framework assumes the DLVO interactions to be between smooth and regular surfaces. In reality, roughness and shape effects should be considered and incorporated requiring more in-depth understanding. Additionally, our theoretical framework does not cover non-DLVO interactions such as the solvation and hydration forces (Butt et al, 2013). However, our findings highlight that some of these types of interactions, e.g. the hydrophobic interaction (sometimes also called the hydrophobic force) found in other papers (Yoon & Mao, 1996; Pan & Yoon, 2016) could be explained by van der Waals type of interactions through applying the Hamaker constant calculations for layered systems.

#### 4. Conclusions

By selecting a flotation-relevant material system, it was shown how surfactant layers can explain the possible attachment of originally hydrophilic systems within the frame of the classic DLVO theory. The energy barrier was already significantly lowered by applying a surfactant layer only. An additional surface gas IGE layer lowers the present energy barrier further but is not mandatory to explain the hydrophobic character of the solid interface. With the help of the proposed model, we were able to explain the particle and bubble size effects within such a flotation system regarding the attachment sub-process. The additional discussed system-relevant effects (e.g. bubble loading capacity, velocity correction, and bubble size correction) are being implemented in a flotation attachment model framework developed recently.

#### Acknowledgments

M. Buchmann was funded through European Union's Horizon 2020 research and innovation program under grant agreement No 821265, project Fine Future. G. Öktem is funded through European Union's Horizon 2020 MSCA-ITN-EID funding, under grant agreement No 955805, project FlotSim.

In honor of 40 years of scientific work, the authors would like to acknowledge the great achievements of Prof. Mehmet S. Çelik in broad fields and on various levels of mineral processing and especially flotation research. We are happy and proud to have Prof. Çelik and his wonderful colleagues at Istanbul Technical University as our collaborators, colleagues, and friends in the EU FineFuture project (2019-2022).

We kindly thank the anonymous reviewers involved with this manuscript for very valuable and constructive requests and discussions which helped to improve the manuscript significantly after the first submission.

## References

- ALBIJANIC, B., AMINI, E., WIGHTMAN, E., OZDEMIR, O., NGUYEN, A. V., BRADSHAW, D. J., 2011, A relationship between the bubble-particle attachment time and the mineralogy of a copper-sulphide ore, *Minerals Engineering*. 24(12), 1335–1339.
- ALBIJANIC, B., BRADSHAW, D. J., NGUYEN, A. V., 2012, The relationships between the bubble-particle attachment time, collector dosage and the mineralogy of a copper sulfide ore, *Minerals Engineering*. 36–38, 309–313.
- ALBIJANIC, B., NIMAL SUBASINGHE, G. K., BRADSHAW, D. J., NGUYEN, A. V., 2015, Influence of liberation on bubble-particle attachment time in flotation, *Minerals Engineering*. 74, 156–162.
- BUTT, H. J., GRAF, K., KAPPL, M., 2003, *Physics and Chemistry of Interfaces*, Wiley-VCH GmbH & Co. KGaA.
- CARNIE, S. L., CHAN, D. Y. C., 1993, Interaction Free Energy between Plate with Charge Regulation, *Journal of Colloid and Interface Science*. 161, 260–264.
- CHAN, D., HEALY, T. W., WHITE, L. R., 1976, Electrical double layer interactions under regulation by surface ionization equilibria-dissimilar amphoteric surfaces, *Journal of the Chemical Society, Faraday Transactions 1: Physical Chemistry in Condensed Phases*. 72, 2844–2865.
- DAI, Z., FORNASIERO, D., RALSTON, J., 1999, Particle-Bubble Attachment in Flotation, *Journal of Colloid and Interface Science*. 217, 70–76.
- DOSHI, D. A., WATKINS, E. B., ISRAELACHVILI, J. N., MAJEWSKI, J., 2005, Reduced water density at hydrophobic surfaces: Effect of dissolved gases, *Proceedings of the National Academy of Sciences of the United States of America*. 102(27), 9458–9462.
- FOUCAUD, Y., LAINÉ, J., FILIPPOV, L. O., BARRÈS, O., KIM, W. J., FILIPPOVA, I. V., PASTORE, M., LEBÈGUE, S., BADAWI, M., 2021, *Adsorption mechanisms of fatty acids on fluorite unraveled by infrared spectroscopy and first-principles calculations*, *Journal of Colloid and Interface Science*. 583, 692–703.
- GRANO, S., 2009, *The critical importance of the grinding environment on fine particle recovery in flotation*, *Minerals Engineering*. 22(4), 386–394.
- GRASSO, D., SUBRAMANIAM, K., BUTKUS, M., STREVETT, K., BERGENDAHL, J., 2002, *A review of non-DLVO interactions in environmental colloidal systems* In: *Re/Views in Environmental Science & Bio/Technology* (Vol. 1).
- GUVEN, O., OZDEMIR, O., KARAAGACLIOGLU, I. E., ÇELİK, M. S., 2015, *Surface morphologies and floatability of sand-blasted quartz particles*, *Minerals Engineering*. 70, 1–7.
- HOGG, R., HEALY, T. W., FUERSTENAU, D. W., 1966, *Mutual coagulation of colloidal dispersions*, *Transactions of the Faraday Society*. 62, 1638–1651.
- JAMESON, G. J., 2012, *The effect of surface liberation and particle size on flotation rate constants*, *Minerals Engineering*. 36–38, 132–137.
- JOSEPH-SOLY, S., QUAST, K., CONNOR, J. N., 2015, *Effects of Eh and pH on the oleate flotation of iron oxides*, *Minerals Engineering*. 83, 97–104.
- KOSIOR, D., ZAWALA, J., NIECIKOWSKA, A., MALYSA, K., 2015, *Influence of non-ionic and ionic surfactants on kinetics of the bubble attachment to hydrophilic and hydrophobic solids*, *Colloids and Surfaces A: Physicochemical and Engineering Aspects*. 470, 333–341.
- KOSIOR, D., ZAWALA, J., TODOROV, R., EXEROWA, D., MALYSA, K., 2014, *Bubble bouncing and stability of liquid films formed under dynamic and static conditions from n-octanol solutions*, *Colloids and Surfaces A: Physicochemical and Engineering Aspects*. 460, 391–400.
- KRASOWSKA, M., MALYSA, K., 2007a, *Kinetics of bubble collision and attachment to hydrophobic solids: I. Effect of surface roughness*, *International Journal of Mineral Processing*. 81(4), 205–216.
- KRASOWSKA, M., MALYSA, K., 2007b, *Wetting films in attachment of the colliding bubble*, *Advances in Colloid and Interface Science*. 134–135, 138–150.
- KRASOWSKA, MARTA, MALYSA, K., BEATTIE, D. A., 2019, *Recent advances in studies of bubble-solid interactions and wetting film stability*, *Current Opinion in Colloid and Interface Science*. 44, 48–58.
- LI, S., NGUYEN, A. V., SUN, Z., 2020, *Stochastic induction time of attachment due to the formation of transient holes in the intervening water films between air bubbles and solid surfaces*, *Journal of Colloid and Interface Science*. 565, 345–350.

- LIFSHITZ, E. M., 1956, *The theory of molecular attractive forces between solids*, Soviet Physics JETP 2, Part 1. 73, 329–349.
- LYKLEMA, J., DUVAL, J. F. L., 2005, *Hetero-interaction between Gouy-Stern double layers: Charge and potential regulation*, Advances in Colloid and Interface Science. 114–115, 27–45.
- MA, M., 2012, *Froth Flotation of Iron Ores*, International Journal of Mining Engineering and Mineral Processing. 1(2), 56–61.
- MISHCHUK, N. A., 2011, *The model of hydrophobic attraction in the framework of classical DLVO forces*, Advances in Colloid and Interface Science. 168(1–2), 149–166.
- MISHCHUK, N., RALSTON, J., FORNASIERO, D., 2006, *Influence of very small bubbles on particle/bubble heterocoagulation*, Journal of Colloid and Interface Science. 301(1), 168–175.
- MITTAL, J., HUMMER, G., 2008, *Static and dynamic correlations in water at hydrophobic interfaces*, Proceedings of the National Academy of Sciences of the United States of America. 105(51), 20130–20135.
- NEETHLING, S. J., BRITO-PARADA, P. R., HADLER, K., CILLIERS, J. J., 2019, *The transition from first to zero order flotation kinetics and its implications for the efficiency of large flotation cells*, Minerals Engineering. 132, 149–161.
- NEETHLING, S. J., CILLIERS, J. J., 2003, *Modelling flotation froths*, International Journal of Mineral Processing. 72(1–4), 267–287.
- NIECIKOWSKA, A., KRASOWSKA, M., RALSTON, J., MALYSA, K., 2012, *Role of surface charge and hydrophobicity in the three-phase contact formation and wetting film stability under dynamic conditions*, Journal of Physical Chemistry C. 116(4), 3071–3078.
- NINHAM, B. W., PARSEGAN, V. A., 1970, *van der Waals Forces: Special Characteristics in Lipid-Water Systems and a General Method of Calculation Based on the Lifshitz Theory*, Biophysical Journal. 10(7), 646–663.
- OCTOBER, L. L., CORIN, K. C., MANONO, M. S., SCHREITHOFER, N., WIESE, J. G., 2020, *A fundamental study considering specific ion effects on the attachment of sulfide minerals to air bubbles*, Minerals Engineering. 151, 106313.
- PAN, L., YOON, R. H., 2016, *Measurement of hydrophobic forces in thin liquid films of water between bubbles and xanthate-treated gold surfaces*, Minerals Engineering. 98, 240–250.
- PARSEGAN, V. A., 2006, *Van der Waals Forces: A Handbook for Biologists, Chemists, Engineers and Physicists*, In Cambridge University Press. Cambridge University Press.
- PARSEGAN, V. A., NINHAM, B. W., 1973, *van der Waals Forces in Many-layered Structures: Generalizations of the Lifshitz Result for two Semi-infinite Media*, J. Theor. Biol. 38, 101–109.
- PATTANAIK, A., VENUGOPAL, R., 2018, *Investigation of Adsorption Mechanism of Reagents (Surfactants) System and its Applicability in Iron Ore Flotation – An Overview*, Colloids and Interface Science Communications. 25, 41–65.
- RATH, S. S., SINHA, N., SAHOO, H., DAS, B., MISHRA, B. K., 2014, *Molecular modeling studies of oleate adsorption on iron oxides*, Applied Surface Science. 295, 115–122.
- SARVARAMINI, A., LARACHI, F., HART, B., 2016, *Collector attachment to lead-activated sphalerite - Experiments and DFT study on pH and solvent effects*, Applied Surface Science. 367, 459–472.
- SCHWARZ, M. P., KOH, P. T. L., VERRELLI, D. I., FENG, Y., 2016, *Sequential multi-scale modelling of mineral processing operations, with application to flotation cells*, Minerals Engineering. 90, 2–16.
- SNOSWELL, D. R. E., DUAN, J., FORNASIERO, D., RALSTON, J., 2003, *Colloid stability and the influence of dissolved gas*, Journal of Physical Chemistry B. 107(13), 2986–2994.
- TANG, Y., YIN, W., KELEBEK, S., 2020, *Magnesite-dolomite separation using potassium cetyl phosphate as a novel flotation collector and related surface chemistry*, Applied Surface Science. 508, 1415191.
- VAZIRI HASSAS, B., CALISKAN, H., GUVEN, O., KARAKAS, F., CINAR, M., CELIK, M. S., 2016, *Effect of roughness and shape factor on flotation characteristics of glass beads*, Colloids and Surfaces A: Physicochemical and Engineering Aspects. 492, 88–99.
- VRIJ, A., OVERBEEK, J. T. H. G., 1968, *Rupture of thin liquid films due to spontaneous fluctuations in thickness*, Journal of the American Chemical Society. 90(12), 3074–3078.
- WANG, XIANCHEN, ZHANG, Q., 2020, *Role of surface roughness in the wettability, surface energy and flotation kinetics of calcite*, Powder Technology. 371, 55–63.
- WANG, XUMING, YIN, X., NALASKOWSKI, J., DU, H., MILLER, J. D., 2015, *Molecular features of water films created with bubbles at silica surfaces*, Surface Innovations. 3(1), 20–26.
- WEBER, C., KNÜPFER, P., BUCHMANN, M., RUDOLPH, M., PEUKER, U. A., 2021, *A comparison between approaches for the calculation of van der Waals interactions in flotation systems*, Minerals Engineering. 167, 106804.
- WIERTEL-POCHOPIEN, A., ZAWALA, J., 2019, *Rupture of Wetting Films Formed by Bubbles at a Quartz Surface in Cationic Surfactant Solutions*, Chemical Engineering and Technology. 42(7), 1371–1380.

- XING, Y., GUI, X., CAO, Y., 2017, *Effect of bubble size on bubble-particle attachment and film drainage kinetics - A theoretical study*, Powder Technology. 322, 140-146.
- YANG, H., XING, Y., SUN, L., CAO, Y., GUI, X., 2020, *Kinetics of bubble-particle attachment and detachment at a single-bubble scale*, Powder Technology. 370, 251-258.
- YOON, R.-H., MAO, L., 1996, *Application of Extended DLVO Theory, IV. Derivation of Flotation Rate Equation from First Principles*. Journal of Colloid and Interface Science. 181, 613-626.
- ZAWALA, J., KARAGUZEL, C., WIERTEL, A., SAHBAZ, O., MALYSA, K., 2017, *Kinetics of the bubble attachment and quartz flotation in mixed solutions of cationic and non-ionic surface-active substances*, Colloids and Surfaces A: Physicochemical and Engineering Aspects. 523, 118-126.
- ZAWALA, JAN, MALYSA, K., KOWALCZUK, P. B., 2020, *On importance of external conditions and properties of the interacting phases in formation and stability of symmetrical and unsymmetrical liquid films*, Advances in Colloid and Interface Science. 276, 102085.
- ZHANG, X., HAN, Y., KAWATRA, S. K., 2021, *Effects of Grinding Media on Grinding Products and Flotation Performance of Sulfide Ores*, Mineral Processing and Extractive Metallurgy Review. 42(3), 172-183.
- ZHU, Z., YIN, W., HAN, H., CAO, S., YANG, B., WANG, D., 2020, *Investigation on the influence of surface roughness on magnetite flotation from the view of both particle-particle and bubble-particle interactions*, Colloids and Surfaces A: Physicochemical and Engineering Aspects. 595, 124681.